Diapiric ascent of silicic magma beneath the Bolivian Altiplano

Rodrigo del Potro,[1] Mikel Díez,[1] Jon Blundy,[1] Antonio G. Camacho,[2] and Joachim Gottsmann[1]

Received 12 April 2013; accepted 18 April 2013; published 31 May 2013.

[1] The vertical transport of large volumes of silicic magma, which drives volcanic eruptions and the long-term compositional evolution of the continental crust, is a highly debated problem. In recent years, dyking has been favored as the main ascent mechanism, but the structural connection between a distributed configuration of melt-filled pores in the source region and shallow magma reservoirs remains unsolved. In the Central Andes, inversion of a new high-resolution Bouguer anomaly data over the Altiplano-Puna Magma Body (APMB) reveals ~15 km wide, vertically elongated, low-density, 3D structures rooted at the top of the APMB at 20 km depth. We integrate our gravity inversion with the available geophysical, geological, and petrological observations, and in agreement with petrological/mechanical considerations propose that, in this region of the Andes, partially molten granitic bodies ascend diapirically through the hot ductile mid-upper crust. **Citation:** del Potro, R., M. Díez, J. Blundy, A. G. Camacho, and J. Gottsmann (2013), Diapiric ascent of silicic magma beneath the Bolivian Altiplano, *Geophys. Res. Lett.*, *40*, 2044–2048, doi:10.1002/grl.50493.

1. The Altiplano-Puna Region

[2] The Altiplano-Puna plateau in the Central Andes is a remarkable location in which to study partially molten bodies in the Earth's crust and their relationship to large volcanic provinces. The thickened continental crust of the Central Andes hosts the Altiplano-Puna Magma Body (APMB), the largest known active, continental, midcrustal zone of partial melt [*Chmielowski et al.*, 1999; *Leidig and Zandt*, 2003; *Schilling et al.*, 2006; *Yuan et al.*, 2000]. Directly above it, the Altiplano-Puna Volcanic Complex (APVC) is the largest Neogene ignimbrite province with a total erupted volume of >12000 km^3, generated mostly in episodic, supervolcanic (volcanic explosivity index, ≥8) eruptions during a "flare-up event" [*de Silva and Gosnold*, 2007]. Despite the waning of ignimbrite activity over the past 2 million years [*Salisbury et al.*, 2011], current signs of unrest are evidenced by large, decade-long, deep-sourced ground deformation at Uturuncu volcano, comprising constant-velocity central uplift and a peripheral subsidence [*Fialko and Pearse*, 2012]. APVC magmas are monotonous, well-mixed hybrids of crustal melts (50%–80%) and more mafic arc magmas (20%–50%), with remarkably constant petrological and geochemical characteristics, thought to have a common origin at the APMB [*de Silva*, 1989; *Ort et al.*, 1996]. The APMB has been identified as a first-order geophysical anomaly by independent seismic [*Chmielowski et al.*, 1999; *Leidig and Zandt*, 2003; *Schurr et al.*, 2003; *Yuan et al.*, 2000], magnetotelluric [*Brasse et al.*, 2002], and gravity surveys [*Gotze and Kirchner*, 1997]. It is characterized by low seismic velocities, very high conductivity, and low density; integration of these different data sets requires the presence of a 15–30 vol.% interconnected melt in the APMB [*Schilling et al.*, 2006]. This is consistent with the observed high heat flux [*Springer and Forster*, 1998], shallow brittle-ductile transition zone (BDTZ) [*de Silva and Gosnold*, 2007; *Jay et al.*, 2012], and a strong crustal anisotropy, possibly caused by a system of fluid-filled cracks above the APMB [*Leidig and Zandt*, 2003]. The top of the APMB is well defined at ~14–20 km below the surface [*Leidig and Zandt*, 2003; *Schilling et al.*, 2006], whereas estimates of its thickness range from ~1 km [*Chmielowski et al.*, 1999; *Leidig and Zandt*, 2003] to 10–20 km [*Yuan et al.*, 2000] to suggestions that it could reach the Moho [*Schurr et al.*, 2003].

2. Gravity Survey and Data Inversion

[3] Previous regional gravity surveys (AnGrav) detected a strong negative Bouguer anomaly associated with the APMB, with a −50 mGal residual in the isostatic and modeled residual anomalies [*Prezzi et al.*, 2009], interpreted as the combined effect of low-density volcaniclastics and partial melt [*Gotze and Kirchner*, 1997; *Prezzi et al.*, 2009]. In this study (GravUt), we increased the extent and resolution of gravity surveys above the APMB (Figure 1a); details of the survey setup and data reduction are given in online supplement. The Bouguer anomaly (Figure 1b) shows a strong, elongated, 40 km wide low along the eastern flank of the active volcanic arc and an even stronger, ~130 km long, ~80 km wide, long wavelength low east of the volcanic arc, which correlates with the largest *Ps*/*P* ratios [*Yuan et al.*, 2000].

[4] We assume the gravity anomaly is generated within the crust and invert the new gravity data for the subsurface density structure using GROWTH2.0 [*Camacho et al.*, 2011], a 3D, automatic, nonsubjective routine that builds a local anomaly model based on controlled "growth" of bodies with prescribed density contrast, by means of an exploratory approach. We invert for a full range of plausible density contrasts, from ±30 to ±400 kg m^{-3} and for a full range of regional gravity components (see details in online supplement). We assume a homogeneous density profile for the bulk of the upper crust because seismic velocity studies show no evidence for density stratification or sharp

Additional supporting information may be found in the online version of this article.

[1]School of Earth Sciences, University of Bristol, Bristol, UK.
[2]Instituto de Geociencias, Centro Mixto del Consejo Superior de Investigaciones Científicas y de la Universidad Complutense de Madrid, Madrid, Spain.

Corresponding author: R. del Potro, School of Earth Sciences, University of Bristol, BS8 1RJ, Bristol, UK. (r.delpotro@bristol.ac.uk)

0094-8276/13/10.1002/grl.50493

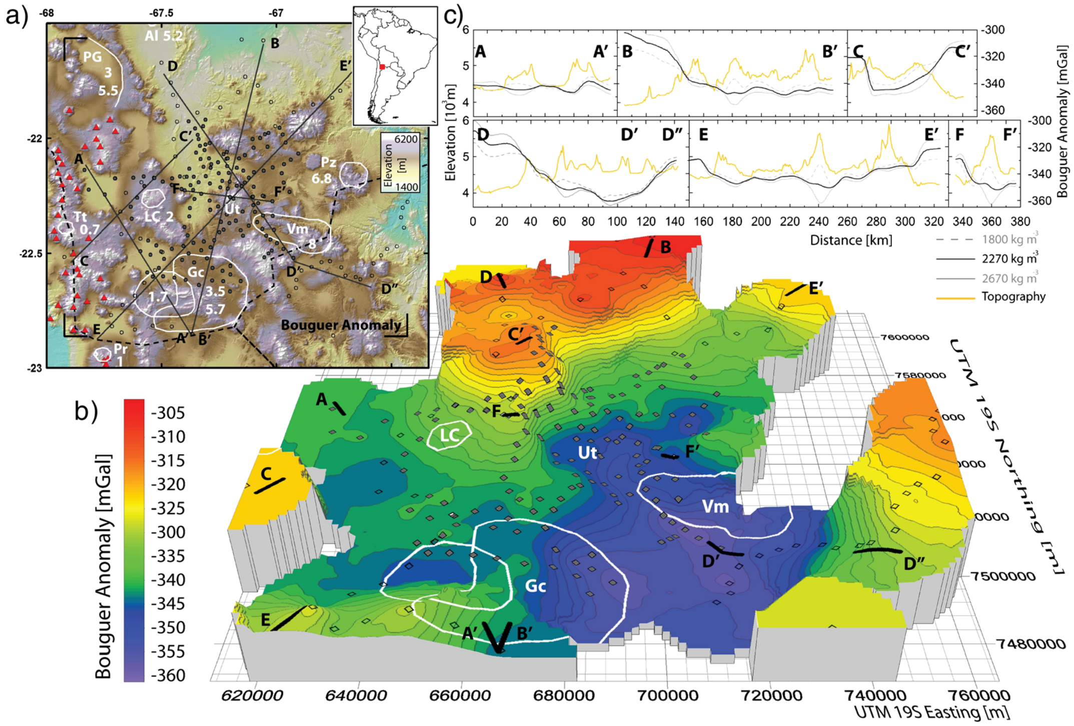

Figure 1. (a) Topography of the APVC showing the location of the AnGrav (open circles) and GravUt (gray circles) gravity stations, national boundaries (dashed black line), Quaternary volcanoes (red triangles) and main Neogene calderas (white lines) [*Salisbury et al.*, 2011]. Al: Alota, PG: Pastos Grandes, LC: Laguna Colorada, Tt: Tatio, Pz: Panizos, Vm: Vilama, Gc: Guacha and Pr: Purico. Numbers indicate date of eruptions in Myr ago. Ut shows the location of Uturuncu volcano. Black lines and letters indicate the location of the profiles shown in Figure 1c. (b) 3D view of the Bouguer anomaly map, with 2 mGal contours, for a reduction density of 2270 kg m^{-3}. (c) Profiles through the Bouguer anomaly and the topography for different normalised reduction densities.

variations between sea level and the top of the APMB [*Chmielowski et al.*, 1999; *Leidig and Zandt*, 2003].

[5] The resultant 3D inversions show persistent anomalous negative gravity structures that extend beyond the published depth of the APMB (Figure 2). Deep, first-order anomalous structures east of the volcanic arc are aligned NE-SW, in agreement with seismic anisotropy [*Leidig and Zandt*, 2003]. Near the top of the APMB and beneath the volcanic arc, these structures comprise NW-SE elongated ridges which are aligned subparallel to the crustal scale NW-SE trending Lípez Fault Zone (~21°S–23°S) of left lateral transtension [*Riller et al.*, 2001]. At shallower levels, these ridges develop into six equidimensional domes, 12–20 km in diameter and with a 25–40 km interspacing. Remarkably, the anomalous bodies show no spatial correlation with the Neogene caldera systems (Figure S3). One body, however, correlates with the ground deformation signal over Uturuncu and correlates spatially with surface thermal anomalies. We find similar results for the entire density parameter space explored in the inversions (Figure S1).

[6] The observed gravity anomaly requires a density contrast in excess of 30 kg m^{-3} (Figure 3), which rules out thermal expansion as the sole cause of the mass deficiency at depth. Similarly, the depth and shape of the anomalous bodies precludes the presence of unconsolidated volcaniclastics and/or hydrothermal systems as the main cause. The mass deficiency may arise from the presence of plutons and/or melt. Petrological data [*Lucassen et al.*, 2001; *Sparks et al.*, 2008] and geophysical constraints [*Prezzi et al.*, 2009; *Zandt et al.*, 1994] establish the overall density of the mid-upper crust to be 2700 kg m^{-3}, while the Bouguer anomaly data constrain the possible range of density contrasts and relative volumes of the anomalous bodies for different size inversion grids (Figure 3 and online supplement). In one possible scenario, the anomalous bodies would represent crystallized granitoids in the mid-upper crust. These granitoids, with the composition of the Uturuncu dacites [*Sparks et al.*, 2008], would have a density of 2650 kg m^{-3} and hence a small density contrast with the host. In order to fit the Bouguer anomaly, they would comprise a minimum ~25% of the total volume (Figure 3), and their geometry would greatly differ from the expected flat or wedge shape of silicic intrusions with small root zones or feeder channels [*Cruden and McCaffrey*, 2001; *McCaffrey and Petford*, 1997; *Petford et al.*, 2000] (Figure 2c). While modest-scale ballooning of a magma reservoir could lead to steep-sided, vertically elongated pluton geometries, with upward concentration of evolved melt and volatiles that generate ignimbrite eruptions [*Lipman*, 2007], one would expect a spatial correlation between the plutons and calderas without any associated ground deformation signal, however, such correlation is lacking. Thus, either magma reservoirs beneath the calderas were almost fully evacuated during the paroxysms or the crystallized remnants have no density contrast with the host.

[7] An alternative scenario arises from larger modeled density contrasts (Figure 2a and b), which produce smaller volumes of anomalous bodies and imply the presence of a melt fraction as the cause of the observed mass deficiency (Figure 3, red region). If these domes are partially molten and have a high

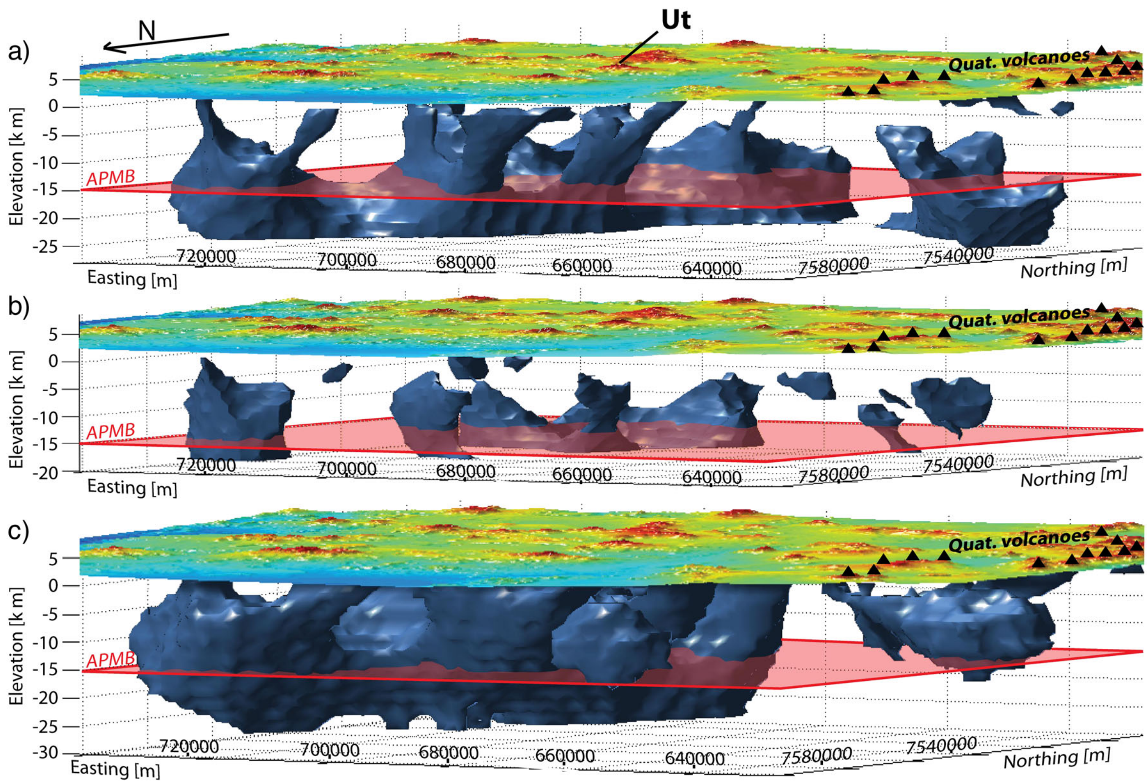

Figure 2. Oblique 3D views, looking ESE, of the modeled negative anomalous bodies (blue regions) for three different density contrasts: (a) -150 kg m^{-3}, (b) -400 kg m^{-3}, and (c) -70 kg m^{-3}. Figure 3 shows the volume of melt associated to each of the three models (25%, 95%, and 0%, respectively), following petrologically based scenarios. The red surfaces indicate the published depth of the top of the APMB. The anomaly beneath Uturuncu volcano (Ut) is deemed responsible for the uplift signal measured at the surface.

buoyancy, they could be causing the surface ground deformation observed by *Fialko and Pearse* [2012]. A key question is the nature of the melt phase. We examine different petrological scenarios using the compositional range of magmas erupted from Uturuncu volcano [*Sparks et al.*, 2008] and the algorithms of *Ochs and Lange* [1999] and *Hacker and Abers* [2004] to calculate physical properties (see online supplement). At one extreme, we consider 100% dacitic melt

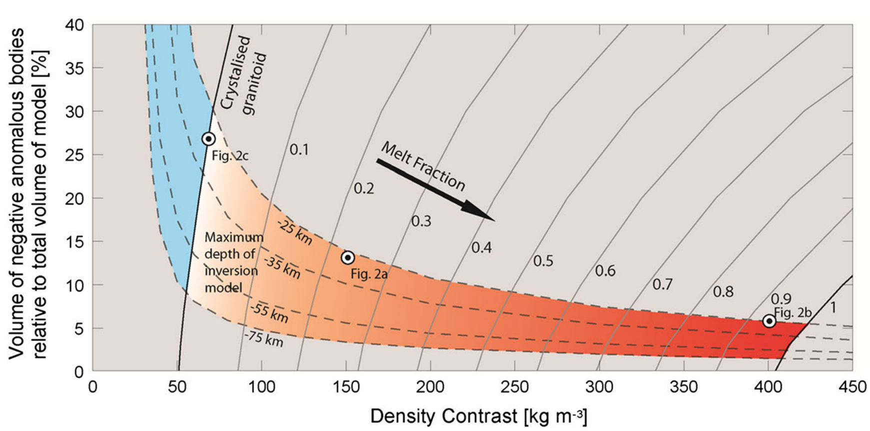

Figure 3. Plot showing the volume-density relationship constrained from the inversion of the Bouguer anomaly for different maximum depths of the anomalous bodies (dashed lines). The volume-density relationship is also shown for an overall crustal density of 2700 kg m^{-3} comprising a dacitic mixture, with varying melt fractions (where the two end members are: dacitic melt 2300 kg m^{-3} and crystallized dacite 2650 kg m^{-3}) within a felsic crust (solid lines). See online supplement for details. These constraints delimit the range of plausible scenarios: the blue shaded area corresponds to crystallized plutons, whereas the red-graded area corresponds to partially molten bodies. The three dots correspond to the scenarios in Figure 2.

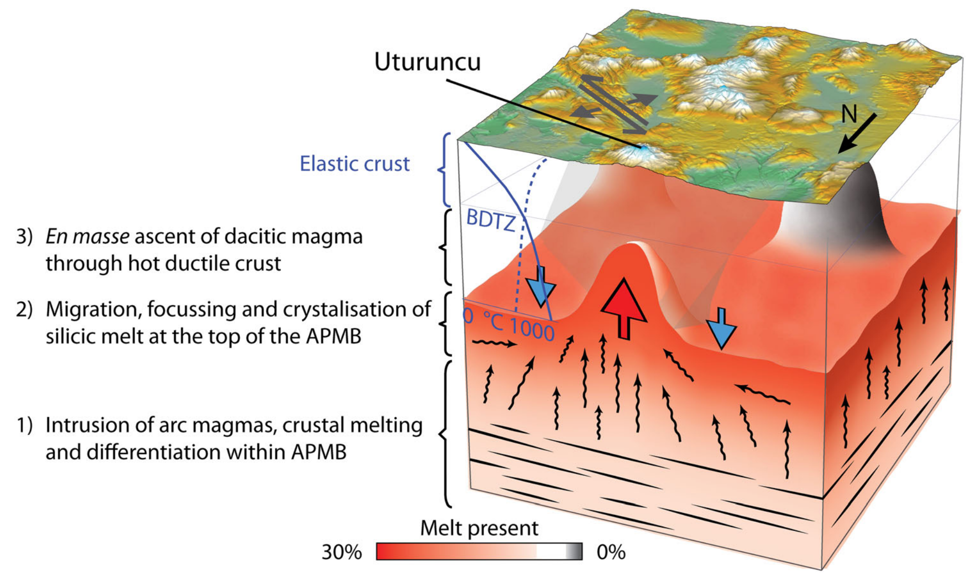

Figure 4. Sketch of the processes inferred to be taking place in the mid-upper crust beneath the APVC. See main text for a detailed explanation. Black arrows represent migration of residual dacitic melt generated by differentiation of andesitic parent magmas, and horizontal lines denote compacted cumulates. The gray plane and arrows represent zones of left lateral transtension, which may intercept the APMB at depth [*Riller et al*., 2001]. The blue solid line indicates the perturbed geotherm, and the dashed line the solidus of a wet tonalite [*de Silva and Gosnold*, 2007] to illustrate the shallow depth of the current brittle-ductile transition zone (BDTZ) identified by *Jay et al*., [2012]. In this scenario, we suggest active diapiric ascent of magma from the top of the APMB beneath Uturuncu volcano.

(Figures 2b and 3), and at the other extreme a two-phase mixture of dacitic melt and crystallized (solid) dacite (Figures 2a and 3). The latter could arise either from solidification of the melt or from entrained solid fragments. If norite (orthopyroxene + plagioclase) accumulates from parental andesite were included, as observed as xenoliths at Uturuncu [*Sparks et al*., 2008], a melt fraction increase of 50 vol.% is required to produce the same density contrast as the two-phase dacitic mixture (see online supplement). Our preferred model, shown in Figures 2a and 3, is for a density contrast of -150 kg m^{-3}, which corresponds to a solid-liquid mixture with a melt fraction of ~25%, similar to that inferred by other methods for the APMB. However, we emphasize that scenarios within the reddish area in Figure 3 are, in principle, possible and that a more realistic situation would likely involve a combination of crystallized plutons and distributed, partially molten bodies with a range of melt fractions.

3. Magma Ascent Mechanism

[8] On the basis of all available observations, we put forward a geological scenario consistent with well-established physical principles and current mechanical and petrological understanding (Figure 4). We envisage the APMB as the ultimate source of evolved, silica-rich magmas, being a dynamic melt zone into which mantle-derived, hydrous basaltic magmas (and their differentiates) intrude from below, partly crystallize and differentiate, with concomitant partial melting of the overlying crust [*Sparks et al*., 2008]. The APMB therefore contains melts ranging in composition from basalt to dacite with associated crystalline residues. Silicic melts generated in this way are buoyant due to elevated silica and H_2O contents and accumulate at the upper levels of the APMB through gravity-controlled compaction [*Solano et al*., 2012] or deformation-assisted segregation [*Brown and Solar*, 1999; *Stevenson*, 1989] (Figure 4) to create melt-rich regions that are potential locations for the initiation of magma extraction. These melt-rich regions could also be the outcome of tectonomagmatic interactions [*Weinberg*, 1996], such that crustal scale, low-viscosity shear zones intercepting the APMB [*Riller et al*., 2001] could prescribe the initial sites for magma extraction (Figure 4). An observation suggesting that this could be the case is the fact that Neogene volcanic belts are aligned with crustal scale shear zones [*Riller et al*., 2001].

[9] Once enough buoyant magma has accumulated at the top of the APMB, it could initiate ascent *en masse* through gravitational instability if host rocks are hot enough to enable creep flow [*Weinberg and Podladchikov*, 1994], which observations suggest is the case [*Jay et al*., 2012; *Springer and Forster*, 1998]. Dyking is found implausible as a means to connect the APMB, and the shallower level low-density bodies as intrusions fed by dykes would appear as rootless or wedge-shaped structures in the gravity inversion; instead, they consistently appear rooted at the APMB (see online supplement and Figure S4). As magmas that erupted from Uturuncu itself are dacitic in composition [*Sparks et al*., 2008], rather than mixtures of dacitic melt and residual/entrained crystals, we consider that during diapir ascent, further physical and chemical differentiation occurs via the compaction of the diapiric mixture [cf. *Solano et al*., 2012], such that the diapir becomes increasingly melt rich and chemically evolved toward its top.

[10] Although the details of the melt segregation, focusing, and ascent mechanisms remain to be addressed, our gravity data, the well-established presence of the APMB, the temporal and spatial pattern of ground deformation at Uturuncu, and the hot ductile crust suggest that the APMB-APVC setting is conducive to the current diapiric ascent of silicic magmas in the mid-upper crust.

[11] **Acknowledgments.** R. P., J. B. and J. G. are supported by the Natural Environmental Research Council (grant NE/G01843X/1). J. G. is supported by a Royal Society University Research Fellowship. M. D. and J. B. are supported by ERC Advanced Grant “CRITMAG.” A.G.C. is supported by the Spanish MICINN project AYA2010-17448. This research is a contribution to the Moncloa Campus of International Excellence (UCM-UPM, CSIC). NERC-GEF provided instruments through loans 910 and 928. We acknowledge Mayel Sunagua, SERGEOTECMIN, Observatorio San Calixto, Néstor Jiménez, UMSA, and SERNAP for their assistance in Bolivia. We thank Roberto Weinberg and Francisco Gutiérrez Ferrer for their useful reviews.

[12] The Editor thanks Roberto Weinberg and Francisco Gutierrez Ferrer for their assistance in evaluating this paper.

References

Brasse, H., P. Lezaeta, V. Rath, K. Schwalenberg, W. Soyer, and V. Haak (2002), The Bolivian Altiplano conductivity anomaly, *J. Geophys. Res.*, *107*(B5).

Brown, M., and G. S. Solar (1999), The mechanism of ascent and emplacement of granite magma during transpression: A syntectonic granite paradigm, *Tectonophysics*, *312*(1), 1–33.

Camacho, A. G., J. Fernandez, and J. Gottsmann (2011), The 3-D gravity inversion package GROWTH2.0 and its application to Tenerife Island, Spain, *Comput. Geosci.*, *37*(4), 621–633.

Chmielowski, J., G. Zandt, and C. Haberland (1999), The central Andean Altiplano-Puna magma body, *Geophys. Res. Lett.*, *26*(6), 783–786.

Cruden, A. R., and K. J. W. McCaffrey (2001), Growth of plutons by floor subsidence: Implications for rates of emplacement, intrusion spacing and melt-extraction mechanisms, *Phys. Chem. Earth Part A—Solid Earth Geodesy*, *26*(4–5), 303–315.

Fialko, Y., and J. Pearse (2012), Sombrero Uplift Above the Altiplano-Puna Magma Body: Evidence of a Ballooning Mid-Crustal Diapir, *Science*, *338*(6104), 250–252.

Gotze, H. J., and A. Kirchner (1997), Interpretation of gravity and geoid in the Central Andes between 20 degrees and 29 degrees S, *J. South Am. Earth Sci.*, *10*(2), 179–188.

Hacker, B. R., and G. A. Abers (2004), Subduction Factory 3: An Excel worksheet and macro for calculating the densities, seismic wave speeds, and H_2O contents of minerals and rocks at pressure and temperature, *Geochem. Geophys. Geosyst.*, *5*(1), Q01005, doi:10.1029/2003GC000614.

Jay, J., M. Pritchard, M. West, D. Christensen, M. Haney, E. Minaya, M. Sunagua, S. McNutt, and M. Zabala (2012), Shallow seismicity, triggered seismicity, and ambient noise tomography at the long-dormant Uturuncu Volcano, Bolivia, *Bull. Volcanol.*, *74*(4), 817–837.

Leidig, M., and G. Zandt (2003), Modeling of highly anisotropic crust and application to the Altiplano-Puna volcanic complex of the central Andes, *J. Geophys. Res.*, *108*(B1), 2014, doi:10.1029/2001JB000649.

Lipman, P. W. (2007), Incremental assembly and prolonged consolidation of Cordilleran magma chambers: Evidence from the Southern Rocky Mountain volcanic field, *Geosphere*, *3*(1), 42–70.

Lucassen, F., R. Becchio, R. Harmon, S. Kasemann, G. Franz, R. Trumbull, H. G. Wilke, R. L. Romer, and P. Dulski (2001), Composition and density model of the continental crust at an active continental margin - the Central Andes between 21 degrees and 27 degrees S, *Tectonophysics*, *341*(1–4), 195–223.

McCaffrey, K. J. W., and N. Petford (1997), Are granitic intrusions scale invariant?, *J. Geol. Soc.*, *154*(1), 1–4.

Ochs, F. A., and R. A. Lange (1999), The density of hydrous magmatic liquids, *Science*, *283*(5406), 1314–1317.

Ort, M. H., B. L. Coira, and M. M. Mazzoni (1996), Generation of a crust-mantle magma mixture: Magma sources and contamination at Cerro Panizos, central Andes, *Contrib. Mineral. Petrol.*, *123*(3), 308–322.

Petford, N., A. R. Cruden, K. J. W. McCaffrey, and J. L. Vigneresse (2000), Granite magma formation, transport and emplacement in the Earth’s crust, *Nature*, *408*(6813), 669–673.

Prezzi, C. B., H. J. Gotze, and S. Schmidt (2009), 3D density model of the Central Andes, *Phys. Earth Planet. Inter.*, *177*(3–4), 217–234.

Riller, U., I. Petrinovic, J. Ramelow, M. Strecker, and O. Oncken (2001), Late Cenozoic tectonism, collapse caldera and plateau formation in the central Andes, *Earth Planet. Sci. Lett.*, *188*(3–4), 299–311.

Salisbury, M. J., B. R. Jicha, S. L. de Silva, B. S. Singer, N. C. Jimenez, and M. H. Ort (2011), (40)Ar/(39)Ar chronostratigraphy of Altiplano-Puna volcanic complex ignimbrites reveals the development of a major magmatic province, *Geol. Soc. Am. Bull.*, *123*(5–6), 821–840.

Schilling, F. R., et al. (2006), Partial melting in the Central Andean Crust: A review of geophysical, petrophysical, and petrologic evidence, in *The Andes-Active Subduction Orogeny*, edited by O. Oncken, G. Chong, G. Franz, P. Giese, H.-J. Götze, V. Ramos, M. Strecker, and P. Wigger, pp. 459–474, Springer, Berlin and Heidelberg.

Schurr, B., G. Asch, A. Rietbrock, R. Trumbull, and C. Haberland (2003), Complex patterns of fluid and melt transport in the central Andean subduction zone revealed by attenuation tomography, *Earth Planet. Sci. Lett.*, *215*(1–2), 105–119.

de Silva, S. L. (1989), Altiplano-Puna volcanic complex of the central Andes, *Geology*, *17*(12), 1102–1106.

de Silva, S. L., and W. D. Gosnold (2007), Episodic construction of batholiths: Insights from the spatiotemporal development of an ignimbrite flare-up, *J. Volcanol. Geotherm. Res.*, *167*(1–4), 320–335.

Solano, J. M. S., M. D. Jackson, R. S. J. Sparks, J. D. Blundy, and C. Annen (2012), Melt segregation in deep crustal hot zones: A mechanism for chemical differentiation, crustal assimilation and the formation of evolved magmas, *J. Petrol.*, *53*(10), 1999–2026.

Sparks, R. S. J., C. B. Folkes, M. C. S. Humphreys, D. N. Barfod, J. Clavero, M. C. Sunagua, S. R. McNutt, and M. E. Pritchard (2008), Uturuncu volcano, Bolivia: Volcanic unrest due to mid-crustal magma intrusion, *Am. J. Sci.*, *308*(6), 727–769.

Springer, M., and A. Forster (1998), Heat-flow density across the Central Andean subduction zone, *Tectonophysics*, *291*(1–4), 123–139.

Stevenson, D. J. (1989), Spontaneous small-scale melt segregation in partial melts undergoing deformation, *Geophys. Res. Lett.*, *16*(9), 1067–1070.

Weinberg, R. F. (1996), Ascent mechanism of felsic magmas: News and views, *Trans. Royal Soc. Edinburgh Earth Sci.*, *87*, 95–103.

Weinberg, R. F., and Y. Podladchikov (1994), Diapiric ascent of magmas through power law crust and mantle, *J. Geophys. Res.*, *99*(B5), 9543–9559.

Yuan, X., et al. (2000), Subduction and collision processes in the Central Andes constrained by converted seismic phases, *Nature*, *408*(6815), 958–961.

Zandt, G., A. A. Valasco, and S. L. Beck (1994), Composition and thickness of the southern Altiplano crust, Bolivia, *Geology*, *22*(11), 1003–1006.